

# Light-ionic fragment production in dissociative electron–molecular-ion collisions: Detection of $D^+$ and $D_2^+$ from $ND_n^+$ ( $n=2-4$ ) and $OD_n^+$ ( $n=2,3$ )

N. Djurić,<sup>1</sup> A. Neau,<sup>1,2</sup> S. Rosén,<sup>1,2</sup> W. Zong,<sup>1,2</sup> and G. H. Dunn<sup>1</sup>

<sup>1</sup>*JILA, University of Colorado and National Institute of Standards and Technology, Boulder, Colorado 80309-0440*

<sup>2</sup>*Department of Physics, Stockholm University, Box 6730, S-113 85 Stockholm, Sweden*

(Received 14 March 2000; published 8 August 2000)

Absolute cross sections are reported for the electron impact dissociative excitation of the deuterated ions  $ND_n^+$  ( $n=2-4$ ) and  $OD_n^+$  ( $n=2,3$ ) from threshold up to 70 eV using a crossed beams technique. The method focuses on measuring light dissociation-product ions from a heavy target. For all studied targets,  $D^+$  formation is the dominant channel, with absolute cross section values in the range of  $(1.3-2) \times 10^{-16} \text{ cm}^2$ , once the initial rise from the threshold is past, continuing to 70 eV. The present measurements for dissociation of  $OD_2^+$  and  $OD_3^+$  yielding  $D^+$  are compared with recent results obtained in the storage ring experiments, these cross sections are found to be in a reasonable agreement within the quoted uncertainties over the part of the energy range where they are expected to be the same. The cross sections for obtaining  $D_2^+$  are about an order of magnitude smaller than the cross sections for  $D^+$  formation from the same targets.

PACS number(s): 34.80.Gs, 34.80.Kw

## I. INTRODUCTION

The polyatomic molecular ions  $ND_n^+$  and  $OD_n^+$  are among ten important ion constituents in dense interstellar clouds [1], and are important as impurities present in edge plasmas of fusion reactors [2]. The water molecule probably has the most important influence on the thermal properties of dense interstellar gas, while the hydronium ion  $OH_3^+$  is particularly important both in radiation damaged systems [3] and in laser discharges [4]; it also appears to be the predominant ion in hydrogen and hydrocarbon flames [5]. The ammonium ion  $ND_4^+$  and its clusters are the dominant ions in the Earth's atmosphere at 10 km and below [6].

Studies of dissociative collisions of electrons with molecular ions have been dominated for decades by the examination of the process of dissociative recombination [7]. Meanwhile, the processes of dissociative excitation and dissociative ionization, which also must be regarded in modeling of these plasma environments, have received less attention [8] and are the subject of this paper.

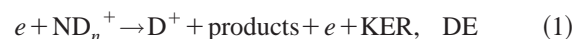
We have previously reported [9,10] dissociation cross sections for obtaining  $D^+$  and  $D_2^+$  from  $CD_n^+$  ( $n=2-5$ ) and have described in some detail the technique for those measurements. We found that the  $D^+$  production channels for  $CD_n^+$  target ions are dominant, with cross sections independent of the number of D atoms ( $n$ ) in the target and with magnitudes of about  $2 \times 10^{-16} \text{ cm}^2$  after the initial rise. In contrast, the channels for production of  $D_2^+$  were about ten times weaker than those for  $D^+$  from the same targets. To investigate this pattern further, we here study the molecular ions  $ND_n^+$  ( $n=2-5$ ) and  $OD_n^+$  ( $n=2,3$ ).

## II. EXPERIMENTAL METHOD

### A. General

Depending on the interaction energy and the shape of potential energy curves, several dissociative processes following electron interactions with a molecular ion could contrib-

ute to the formation of a particular fragment ion. For example, the processes of interest for  $D^+$  production from  $ND_n^+$  target ions may be represented as



where KER is the kinetic energy release for the given process, and the products can be either neutral or charged (positive and negative). Not shown here is the possibility that either the target and/or product ions could be internally excited. These processes are, respectively, called dissociative excitation (DE), which could be direct or resonant excitation (RDE); dissociative ionization (DI); and resonant ion pair formation (RIP). Their respective cross sections are herein denoted by  $\sigma_{\text{DE}}$ ,  $\sigma_{\text{RDE}}$ ,  $\sigma_{\text{DI}}$ , and  $\sigma_{\text{RIP}}$ . The DE and DI processes involve simple excitation of a bound electron to either a dissociative level (DE) or to the electron continuum (DI). RDE and RIP are resonant, two-step processes in which the electron is first captured by the ion into an intermediate state. This doubly excited state of the neutral molecule can stabilize via different competing routes leading to formation of either a pair of charged and neutral fragments (RDE) or to ion pair fragments (RIP).

Our experimental study employs colliding beams of electrons and ions in a crossed beams configuration. The absolute dissociation cross section  $\sigma$  at interaction energy  $E$  for a particular fragmentation process is determined from measured parameters through the relationship [11]

$$\sigma(E) = \frac{Re^2}{I_e I_i} \frac{v_e v_i}{(v_e^2 + v_i^2)^{1/2}} \frac{F}{\epsilon}, \quad (2)$$

where  $R$  is fragment signal count rate,  $v_e$  and  $v_i$  are the electron and ion laboratory velocities,  $I_e$  and  $I_i$  are the currents of electrons and ions, respectively,  $F$  is the form factor

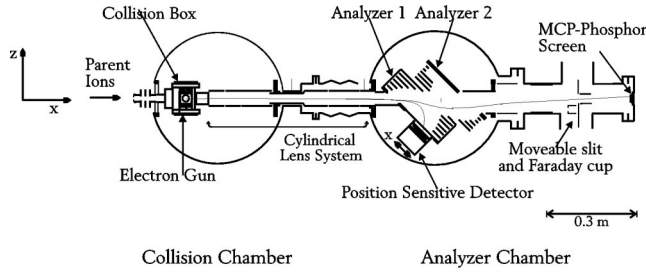


FIG. 1. Crossed electron-ion beams interaction and fragment ion analysis apparatus.

(which takes the spatial overlap of the two beams into account), and  $\epsilon$  is the measured detection efficiency for collection and detection of the studied “signal” ions. The energy scale is calibrated by means of the linear extrapolation method, taking the appearance potential of  $N^{2+}$  from  $N^+$  as 29.6 eV [12].

An experiment consists of measuring the quantities in Eq. (2) and performing sufficient tests to verify that the measurements were correct, that no extraneous effects gave misleading results, and that uncertainties are understood and minimized. Note that the dissociation processes typically result in large spreads in angle and energy, and that since the excess kinetic energy released is predominantly carried away by light dissociation fragments, it is difficult to collect and detect all of the dissociation fragments [9]. Thus, deuterated targets are chosen, because the energy and angular spreads of  $D^+$  fragment ions are smaller than those of  $H^+$  ions (from the isotopomers).

### B. Overview

The JILA apparatus [9] is shown in Fig. 1. The target ions produced from a mixture of  $ND_3(D_2O)$  and  $D_2$  in a dc discharge ion source [13] may be vibrationally and/or electronically excited; it was not possible to control or calculate the state distributions. The ions are extracted, accelerated to 6000 eV energy, mass selected, and directed into the collision chamber where they are intersected at  $90^\circ$  by a magnetically confined (0.006 T) electron beam [14]. The electron beam is chopped at 1000 Hz, and the scalars are gated in an appropriate way in order to separate the true signal produced in the electron-ion collision from background events. A rotatable scanning slit probe is located in the center of the collision box to measure spatial profiles of either the electron or the ion beam. Product ions and parent ions continue through a cylindrically symmetric lens system into the analyzer chamber. The analyzer chamber contains two  $45^\circ$  electrostatic analyzers, a position sensitive detector (PSD), and a set of horizontal deflectors. The first analyzer separates studied fragment ions from the other product ions and from the parent beam, and deflects them onto a 40 mm diameter PSD mounted on a linear motion feedthrough. At the same time, with the help of a second analyzer, the parent ions are redirected toward the electrically isolated small chamber (cross shape, see Fig. 1) where the ion current is measured. Counts from the PSD are registered as a function of the  $x$ - $y$  posi-

tions and time gates in two separate histogram memories so that signal counts can be obtained for all  $x$ - $y$  positions.

As alluded to earlier, fragment ions resulting from the dissociation of the target ions may have several eV of kinetic energy from the dissociation (in the c.m. system), and as a consequence they will have both a larger angular spread and a broader laboratory energy spread than the primary beam [9,10]. The fragment ion distribution at the PSD is found to be relatively narrow in the  $y$  direction (vertical), while in the  $x$  direction (direction of the parent and fragment ions and direction of PSD movement) it is broader and can become so great that not all of the signal ions are detected at a given PSD position. In such a case, we move the PSD to different positions, and obtain final data at a given interaction energy by summing the total signal at one PSD position and then adding the “missing” signal for that position as measured at other PSD positions.

### C. Ion-beam purity

A complication is often present in these studies, arising from the fact that the magnetic analyzer does not separate ions with the same  $m/q$ . For example, the magnet separator will not separate  $ND_4^+$  from  $OD_3^+$ , nor  $ND_3^+$  from  $OD_2^+$ . Hence, a small leak in the gas line or presence of  $H_2O$  as impurity in the source may lead to the contamination of the target beams. The purity of an  $ND_4^+$  or  $ND_3^+$  beam depends on the elimination of water in both the gas manifold and the source plasma, while the purity of the  $OD_3^+$  and  $OD_2^+$  beams relies on the elimination of nitrogen in the gas manifold. A special protocol was developed to keep impurity contents as low as possible. Before  $OD_2$  is introduced in the ion source, it is frozen a few times and nitrogen is pumped from the reservoir. Mass spectra of the primary beam are taken a number of times per day and the ion current ratio  $N_2^+/N^+$  is measured and compared with the ion current of  $OD_2^+$ . When making measurements with  $ND_4^+$  target ions, the source is fed by a mixture of  $N_2$  and  $D_2$  from a reservoir that is kept in a liquid nitrogen trap, to insure that all water present was frozen. Again, mass spectra are taken, this time monitoring  $m/q=17(OH^+)$ . Based on all of these measurements, we deduce that the maximum error introduced in the cross section measurements is about 5%. No correction has been made for this effect, and the 5% error has been included in the systematic uncertainty.

## III. RESULTS AND DISCUSSION

The measured absolute cross sections for  $D^+$  fragment production following electron impact on  $ND_n^+$  ( $n=2-4$ ) and on  $OD_n^+$  ( $n=2,3$ ) are shown in Figs. 2, 3, and 4. The cross sections are relatively smooth functions of energy with very similar absolute magnitudes  $(1.3-2) \times 10^{-16} \text{ cm}^2$ . The strong similarity of the cross sections for isoelectronic species of the same mass, e.g.,  $OD_2^+$  and  $ND_3^+$ , and  $OD_3^+$  and  $ND_4^+$  in shape as well as magnitude, led to our paying extra attention to the above mentioned tests of the ion production system to verify that we did not have contamination.

The independence of the cross section from the number of

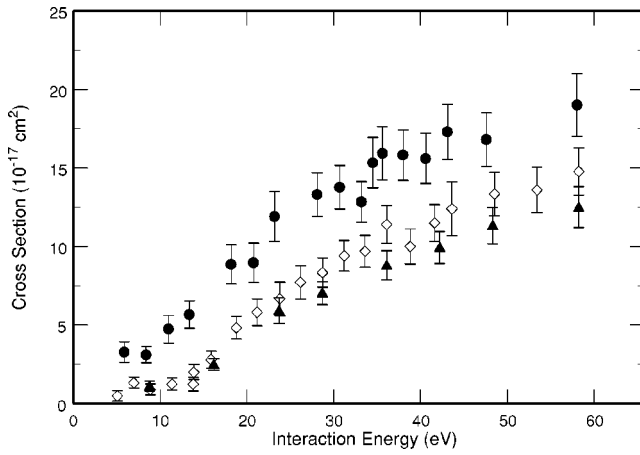


FIG. 2. Absolute cross sections for  $\text{D}^+$  fragment ion production from  $\text{ND}_n^+$ . Points represent average experimental values, and the bars display relative uncertainties at  $1\sigma$  level.  $\blacktriangle$ ,  $\text{ND}_2^+$ ;  $\diamond$ ,  $\text{ND}_3^+$ ;  $\bullet$ ,  $\text{ND}_4^+$ .

D atoms ( $n$ ) in the target was first observed in our earlier studies [10] of  $\text{CD}_n^+$  ( $n=2-5$ ). As one can see from Figs. 2, 3, and 4, a similar phenomenon is observed for the present targets, though one could argue that there is a small dependence on  $n$ , with the cross sections becoming weaker as the number  $n$  gets smaller.

The cross sections for production of  $\text{D}_2^+$  from  $\text{ND}_n^+$  have also been measured and are shown in Fig. 5. Relative uncertainties [15], dominated by fluctuation in the statistical scatter of the data, by the form factor, and by uncertainties in the procedure for summing up the signal at different PSD positions, are shown in the figures at one standard deviation

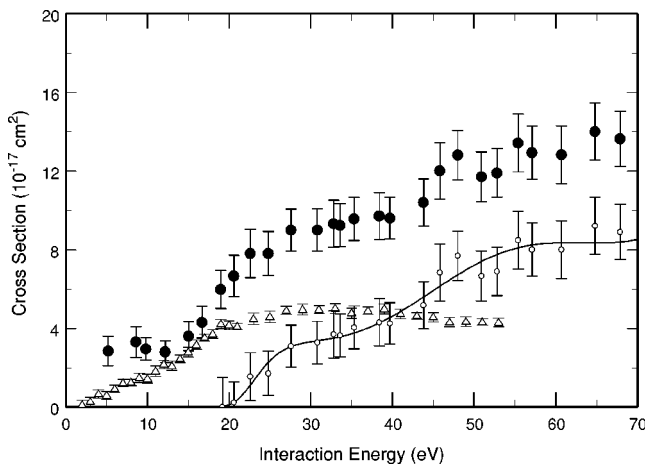


FIG. 3. Absolute cross sections for  $\text{D}^+$  fragment ion production from  $\text{OD}_2^+$ . Solid circles represent average experimental values, and the bars display relative uncertainties at  $1\sigma$  level. Open triangles show the data for obtaining  $\text{OH}$  ( $\text{O}+\text{H}$ ) from  $\text{OH}_2^+$  measured by Jensen *et al.* [17] and the bars represent the uncertainty on the relative scale. The solid line (drawn through the open circles) is an estimate of the dissociative ionization cross section  $\sigma_{\text{DI}}$  (see text) determined by subtracting the data of Jensen *et al.* [17] [fitted with the functional form  $(A/E)\ln E+B$  above 20 eV] from the present data for interaction energies above 20 eV.

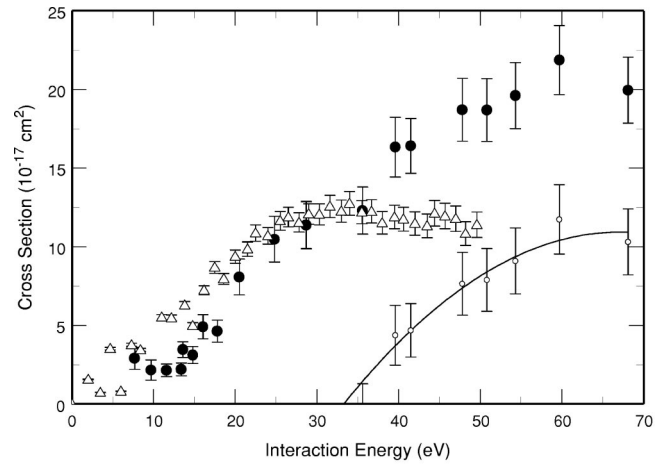


FIG. 4. Absolute cross sections for  $\text{D}^+$  fragment ion production from  $\text{OD}_3^+$ . Solid circles represent average experimental values, and the bars display relative uncertainties at  $1\sigma$  level. Open triangles show the data for obtaining  $\text{OH}_2$  ( $\text{O}+\text{H}+\text{H}$ ) from  $\text{OH}_3^+$  measured by Vejby-Christensen *et al.* [18] and the bars represent the uncertainty on the relative scale. The solid line (drawn through the open circles) is an estimate of the dissociative ionization cross section  $\sigma_{\text{DI}}$  (see text) determined by subtracting the data of Vejby-Christensen *et al.* [18] [fitted with the functional form  $(A/E)\ln E+B$  above 20 eV] from the present data for interaction energies above 20 eV.

$1\sigma$  level. The combined absolute uncertainty  $U$  at the  $1\sigma$  level includes systematic uncertainties, which do not affect the relative shape of the data. These are added in quadrature to the relative uncertainties to obtain the total absolute uncertainty, estimated to be 20% at the  $1\sigma$  level for points near the maximum cross section.

#### A. $\text{ND}_n^+$ ( $n=2-4$ )

Cross sections for dissociation of  $\text{ND}_n^+$  ( $n=2-4$ ) into  $\text{D}^+$  channels are shown in Fig. 2. Calculated proton affinities

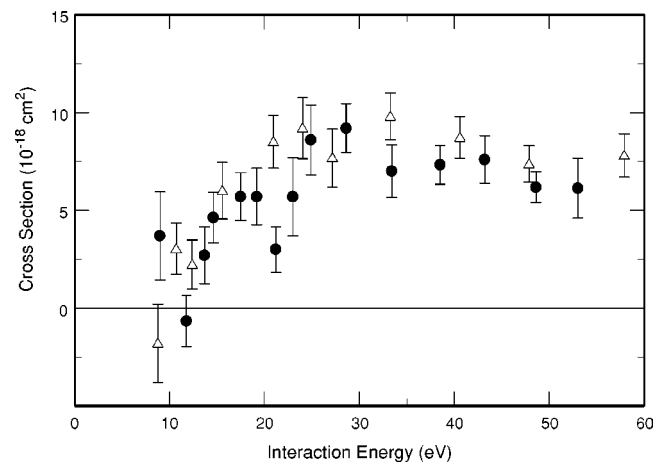


FIG. 5. Absolute cross section measurements for  $\text{D}_2^+$  fragments from  $\text{ND}_n^+$ :  $\bullet$ ,  $\text{ND}_2^+$ ;  $\triangle$ ,  $\text{ND}_3^+$ ;  $\bullet$ ,  $\text{ND}_4^+$ . Points represent average experimental values, and the bars represent relative uncertainties at the  $1\sigma$  level.

[16] for  $\text{NH}$ ,  $\text{NH}_2$ , and  $\text{NH}_3$  are, respectively, 6.2, 8.03, and 8.87 eV. The earlier appearances of  $\text{D}^+$ , below these minimum energies needed for the molecular ions to dissociate, can probably be attributed to a combination of internal excitation of the targets and a contribution from the RIP process. There are no other measurements of dissociation cross sections for  $\text{ND}_n^+$  available for comparison with these present results.

In comparison, the cross sections for producing  $\text{D}_2^+$  (see Fig. 5) are about an order of magnitude smaller than the cross sections for obtaining  $\text{D}^+$  from the same targets. In contrast to our previous measurements [10] on the target ion  $\text{CD}_n^+$  ( $n=2-5$ ), where the channel for  $\text{D}_2^+$  production was dependent on the number of D atoms ( $n$ ) in the target, we find that the cross sections are almost identical for  $\text{ND}_3^+$  and  $\text{ND}_4^+$ .

### B. $\text{OD}_n^+$ ( $n=2,3$ )

The measured cross sections for electron impact dissociation of  $\text{OD}_2^+$  and  $\text{OD}_3^+$  to yield  $\text{D}^+$  are plotted in Figs. 3 and 4 as solid circles. Cross sections rise relatively smoothly from the threshold up to approximately 22 eV, after which there are a few changes in the slope. Such changes in slope can probably be related to the opening of some higher energy dissociation channels contributing to  $\text{D}^+$  production. As in the case of  $\text{ND}_n^+$ , it is difficult to make definitive statements about the appearance potentials of  $\text{D}^+$  from studied  $\text{OD}_n^+$ . First, there is not much information about relevant excited-state repulsive surfaces that correlate to the observed product. Second, the target ions may be internally excited. Therefore, no attempt was made to estimate the appearance potentials of  $\text{D}^+$  or to assign the changes in slope to any specific channel.

#### 1. $\text{OD}_2^+$

In Fig. 3, the measured cross sections for dissociation of  $\text{OD}_2^+$  into  $\text{D}^+$  channels are presented as the solid circles and compared with the recent results of Jensen *et al.* [17] for  $\text{OH}_2^+$ , obtained using a storage ring and detecting the complementary neutral to  $\text{H}^+$ , i.e.,  $\text{OH}$  (open triangles). This comparison is possible because both ions,  $\text{OH}_2^+$  and  $\text{OD}_2^+$ , have the same electronic structure; however, direct comparison is only possible if we assume that in both experiments the targets are in the ground state and that the reaction  $\text{OD}_2^+ + e \rightarrow \text{D}^+ + \text{OD} + e$  is the only one responsible for  $\text{D}^+$  as well as for  $\text{OD}$  production. The experiments performed on the ion storage ring [17] did not distinguish whether the complementary neutral fragment was indeed  $\text{OH}$  or whether it was (partially) fragmented to  $\text{O} + \text{H}$ . The agreement between results is within the quoted absolute uncertainties of the two experiments ( $\pm 25\%$ ) in the threshold region, where one can expect them to be the same. However, there are clearly some discrepancies between the two experiments at higher energies. The cross section measured by Jensen *et al.* [17] reaches a plateau value of approximately  $5 \times 10^{-17} \text{ cm}^2$  at about 19 eV, while the present data continue to rise, reaching the value of approximately  $1.3 \times 10^{-16} \text{ cm}^2$  above 45 eV.

Three dissociation channels are energetically allowed at low energies for dissociation of a ground state  $\text{OD}_2^+$  ion [16]:  $\text{D}^+ + \text{OD}^-$  at 4.32 eV,  $\text{D}^+ + \text{OD} + e$  at 6.15 eV, and  $\text{D}^+ + \text{D} + \text{O} + e$  at 10.58 eV. While the first channel, RIP, can only contribute signal in the present experiment, the last two DE channels will be recorded in both experiments. In both experiments, the measured cross sections appear at energies that are lower than the minimum energies needed for the molecular ion to dissociate, 6.15 eV. In the present experiment, the earlier start of the  $\text{D}^+$  signal is probably due to a combination of the target's being internally excited and a contribution from RIP.

#### 2. $\text{OD}_3^+$

Present results for  $\text{OD}_3^+$  are qualitatively very similar to those for  $\text{OD}_2^+$ . In Fig. 4 our data on  $\text{OD}_3^+$  are compared with the data of Vejby-Christensen *et al.* [18] for  $\text{OH}_3^+$ , obtained using a storage ring experiment and detecting the complementary neutral to  $\text{H}^+$ , i.e.,  $\text{OH}_2$ . The results are in agreement between 5 and 35 eV. Above 35 eV the two curves diverge from each other, thus showing behavior similar to the discussed results on  $\text{OD}_2^+$ . The cross section measured by Vejby-Christensen *et al.* [18] reaches a constant value of approximately  $1.3 \times 10^{-16} \text{ cm}^2$  at about 25 eV, while present data continue to rise, reaching a value of approximately  $2 \times 10^{-16} \text{ cm}^2$  above 50 eV.

Four dissociation channels are energetically allowed at low energies for dissociation of a ground state  $\text{OD}_3^+$  ion [16]:  $\text{D}^+ + \text{OD}_2^-$  at 5.97 eV,  $\text{D}^+ + \text{OD}_2 + e$  at 7.17 eV,  $\text{D}^+ + \text{OD} + \text{D} + e$  at 12.32 eV, and  $\text{D}^+ + \text{D} + \text{D} + \text{O} + e$  at 16.75 eV. As seen in Fig. 4, we measured a nonzero cross section for energies below the minimum dissociation energy of  $\text{OD}_3^+$ , 7.17 eV [16]. Similar to the case of  $\text{OD}_2^+$ , this early appearance of  $\text{D}^+$  may possibly be explained by a combination of the target ions' being internally excited and there being some contributions from RIP.

### C. Dissociative ionization

We now address the differences occurring at higher energies between our crossed beams data and the storage ring results of Jensen *et al.* [17] and Vejby-Christensen *et al.* [18]. One difference between them is that the former detects ions while the latter detects neutrals. Thus the observed discrepancies in measured cross sections for  $\text{D}^+$  formation between 20–70 eV, seen in Figs. 3 and 4, indicate that in this energy range other channels must become allowed that contribute to the  $\text{D}^+$  signal in our experiment but not in the Jensen *et al.* [17] and Vejby-Christensen *et al.* [18] experiments. For example,  $\text{OD}_2^+ + e \rightarrow \text{D}^+ + \text{OD}^+ + 2e$  at 19.18 eV. In the present experiment where  $\text{D}^+$  from  $\text{OD}_2^+$  is detected, the cross section displayed in Fig. 3 is the sum of dissociative excitation ( $\sigma_{\text{DE}} + \sigma_{\text{RDE}}$ ), resonant ion-pair formation  $\sigma_{\text{RIP}}$ , and dissociative ionization  $\sigma_{\text{DI}}$ :

$$\sigma_{\text{tot}} = \sigma_{\text{DE}} + \sigma_{\text{RDE}} + \sigma_{\text{RIP}} + \sigma_{\text{DI}}. \quad (2)$$

In contrast, in the recent measurements by Jensen *et al.* [17], since they detected neutral  $\text{OH}$  (or  $\text{O} + \text{H}$ ) from  $\text{OH}_2^+$  and



did not register fragments from DI or RIP, the cross section is the sum of  $\sigma_{DE} + \sigma_{RDE}$ . Hence, subtraction of data measured by Jensen *et al.* [17] from the present data above 20 eV yields  $\sigma_F = \sigma_{DI} + \sigma_{RIP}$ . Since at these high energies  $\sigma_{RIP}$  is negligible,  $\sigma_F$  is approximately  $\sigma_{DI}$ . We applied the same procedure for analysis of the  $OD_3^+$  and  $OH_3^+$  [18] results, again for energies above 20 eV where new channel such as  $OD_3^+ + e \rightarrow D^+ + OD_2^+ + 2e$  at 19.81 eV [16] become energetically allowed. To perform the subtraction, the results of Jensen *et al.* [17] and Vejby-Christensen *et al.* [18] were first fitted with the functional form  $(A/E)\ln E + B$  and then extrapolated to higher energies. The results of this procedure are shown in Figs. 3 and 4, and they should provide reasonable approximation to  $\sigma_{DI}$ . Of course, this result must be considered with extreme caution because the internal excitation energies of the ion targets can be different in the two experiments, being “hot” in the present experiment and “cold” in the storage ring experiments of Jensen *et al.* [17] and Vejby-Christensen *et al.* [18].

We should point out that both in the comparison of our results for  $OD_2^+$  and  $OD_3^+$  with the results for  $OH_2^+$  [17] and  $OH_3^+$  [18] and in our estimate of the DI, we have ignored any isotope effect. An isotope effect was recently observed in the storage ring experiment of Jensen *et al.* [17] in comparing the DE cross sections of  $OH_2^+$  (OH was detected) and  $OHD^+$  (OH and OD were detected).

#### IV. CONCLUSION

Our technique for measuring light fragment ions in the electron-impact dissociative excitation of small heteronuclear ions produces data complementary to those becoming available from ion storage ring experiments.

Measurements have been performed for electron-impact dissociative excitation of  $ND_n^+$  ions ( $n=2-4$ ) and  $OD_n^+$  ions ( $n=2,3$ ) over an energy range from 4 to 70 eV. The total expanded absolute uncertainty in the results is about 20% at the peak of the cross sections.

Some propensity rules present themselves from both our present and our earlier studies of dissociation of hydrogen bearing molecular ions to yield various hydrogen ions [9,10].

(1) Dissociation of  $ND_n^+$ ,  $OD_n^+$ , and  $CD_n^+$  to yield  $D^+$  produces cross sections nearly independent of the number of D atoms ( $n$ ) in the target and nearly independent of the heavy core.

(2) The magnitude of cross sections for  $D^+$  production from all studied targets is in the range of  $(1.3-2) \times 10^{-16} \text{ cm}^2$  above the threshold.

(3) Dissociation cross sections to produce  $D_2^+$  fragments are about an order of magnitude smaller than those for  $D^+$  production from the same targets.

The dependence of cross sections for  $D_2^+$  production on the number of D atoms ( $n$ ) in the target that was observed in  $CD_n^+$  ( $n=3-5$ ) studies was not observed for  $ND_n^+$  ( $n=3,4$ ); instead the cross sections for different values of  $n$  were almost identical. We have no models or suggested explanations for the listed propensity rules, but we will continue with our efforts to find plausible explanations.

The present measurements for  $OD_n^+$  are compared with those obtained using a storage ring technique for  $OH_2^+$  [17] and  $OH_3^+$  [18] and are found to be in reasonable agreement within the quoted experimental uncertainties over the lower energy range where they are expected to be the same. Outside this energy range, the results have been subtracted from each other to extract an estimate of the dissociative ionization cross section for  $OD_2^+$  and  $OD_3^+$ . In the absence of any direct measurements for DI of molecular ions other than for  $H_2^+$  [19], this indirect approach for estimating DI cross sections yields the only results for these cross sections at present.

#### ACKNOWLEDGMENTS

This work was supported in part by the Office of Fusion Energy of the U.S. Department of Energy under Contract No. DE-A102-95ER54293 with the National Institute of Standards and Technology. This work was also supported by the Swedish Natural Science Research Council, the Gören Gustafson Foundation for Research in Natural Science and Medicine, and the Swedish Foundation for International Cooperation in Research and Higher Education.

- [1] A. Sternberg and A. Delgarno, *Astrophys. J., Suppl. Ser.* **99**, 565 (1995).
- [2] G. H. Dunn, *Nucl. Fusion Suppl.* **2**, 25 (1992).
- [3] J. K. Thomas, *Advanced Radiation Chemistry*, edited by M. Burton and J. Magee (Wiley Interscience, New York, 1969), Vol. 1, p. 103.
- [4] L. J. Denes and J. J. Lowke, *Appl. Phys. Lett.* **23**, 1353 (1981).
- [5] W. J. Miller, *14th International Symposium on Combustion* (The Combustion Institute, Pittsburgh, 1973), p. 307.
- [6] F. C. Fehsenfeld and E. E. Ferguson, *J. Chem. Phys.* **59**, 6272 (1973).
- [7] See, for example, *Dissociative Recombination: Theory, Experiment and Applications IV*, edited by M. Larsson, J. B. A.

- Mitchell, and I. E. Schneider (World Scientific, Singapore, 2000); *Dissociative Recombination: Theory, Experiment and Applications III*, edited by D. Zajfman, J. B. A. Mitchell, D. Schwalm, and B. R. Rowe (World Scientific, Singapore, 1996); M. Larsson, *Annu. Rev. Phys. Chem.* **48**, 151 (1997).
- [8] G. H. Dunn and N. Djurić, in *Novel Aspects of Electron-Molecule Scattering*, edited by K. Becker (World Scientific, Singapore, 1998), pp. 241–281.
- [9] N. Djurić, Y. S. Chung, B. Wallbank, and G. H. Dunn, *Phys. Rev. A* **56**, 2887 (1997).
- [10] N. Djurić, S. Zhou, G. H. Dunn, and M. E. Bannister, *Phys. Rev. A* **58**, 304 (1998).
- [11] G. H. Dunn, in *Electron Impact Ionization*, edited by T. D.

- Märk and G. H. Dunn (Springer-Verlag, New York, 1985), Chap. 8.
- [12] C. E. Moore, *Atomic Energy Levels*, Natl. Bur. Stand. (U.S.) Circ. No. 467 (U. S. GPO, Washington, DC, 1949), Vol. 1.
- [13] M. Menzinger and L. Wählin, *Rev. Sci. Instrum.* **40**, 102 (1969).
- [14] P. O. Taylor, K. T. Dolder, W. E. Kauppila, and G. H. Dunn, *Rev. Sci. Instrum.* **45**, 538 (1974).
- [15] Uncertainties are presented as per the guidelines by B. N. Taylor and C. E. Kuyatt, NIST Technical Report No 1297, 1993 (unpublished).
- [16] *NIST Chemistry WebBook, NIST Standard Reference Database Number 69*, edited by W. G. Mallard and P. J. Linstrom, February 2000 (National Institute of Standards and Technology, Gaithersburg MD, 2000).
- [17] M. J. Jensen, R. C. Bilodeau, O. Heber, H. B. Pedersen, C. P. Safvan, X. Urbain, D. Zajfman, and L. H. Andersen, *Phys. Rev. A* **60**, 2970 (1999).
- [18] L. Vejby-Christensen, L. H. Andersen, O. Heber, D. Kella, H. B. Pedersen, H. T. Schmidt, and D. Zajfman, *Astrophys. J.* **483**, 531 (1997).
- [19] B. Peart and K. T. Dolder, *J. Phys. B* **8**, 1570 (1970).